Major Components of Aerosols in North China: Desert Region and the Yellow Sea in the Spring and Summer of 1995 and 1996

J. ZHANG

State Key Laboratory of Estuarine and Coastal Research, East China Normal University, Shanghai, and College of Chemistry and Chemical Engineering, Ocean University of Qingdao, Qingdao, China

Y. WU

State Key Laboratory of Estuarine and Coastal Research, East China Normal University, Shanghai, China

C. L. LIU

Institute of Marine Geology, Ministry of Geology and Mineral Resources, Qingdao, China

Z. B. SHEN

Lanzhou Institute of Plateau Atmospheric Physics, Chinese Academy of Sciences, Lanzhou, China

Y. ZHANG

IMS, Canadian Centre for Remote Sensing, Ottawa, Ontario, Canada

(Manuscript received 5 October 2000, in final form 1 October 2001)

ABSTRACT

Aerosol samples were collected from the northwest China desert region (i.e., Minqin), a coastal suburb area (i.e., Qingdao), and an island from the Yellow Sea (i.e., Qianliyan), respectively, in spring and summer of 1995 and 1996. Samples were analyzed for major components (Al, Ca, K, Mg, and Na), carbon (RAC), and sulphur (RAS). The results show that concentration of aerosols change considerably in time and space. The application of a three end-member-mixing model indicates that dust-dominated materials contribute up to 80%–90% of total aerosols when the cold fronts pass through over the Yellow Sea. The crust-dominated aerosols carried by cold front systems may well reduce the percentage concentrations of pollutant and sea salt over the Yellow Sea. The sea salt and regional aerosols become dominant fractions in atmosphere in summer when the dust storms expire in desert regions and the southeast monsoon starts in the subtropical Pacific Ocean.

1. Introduction

It is now well recognized that East Asia injects a huge amount of mineral particles into atmosphere associated with cold fronts in spring and early summer each year. These particles, once released into the air, can be transported under westerlies over the North Pacific Ocean at midlatitude. In this context, aerosols blown to the ocean cross a variety of land and marine recipients, and regional/local emission sources impose control over the composition of air mass (Parungo et al. 1994; Chen et al. 1997; Kim et al. 1998). It was indicated that in coastal oceans (e.g., Mediterranean Sea, North Sea, and Irish Sea) the origin of air mass, rather than the marine sampling location, constrains the fingerprint of aerosol compositions (Chester and Bradshaw 1991; Guieu et al. 1997; Chester et al. 2000). Very few data are available to examine this synthesis at the North Pacific Ocean.

The atmosphere of China and the adjacent coastal ocean is strongly influenced by complicated air masses; for example, a Siberia high moves eastward and southward in spring, and the southeast and southwest monsoons blow to the north in summer. Consequently, the wind field over this region is highly variable, but is dominantly southeastward in winter and spring, and northward in summer and autumn. With respect to the coastal seas around China, important progresses have emerged in literature on aerosol compositions (cf. Parungo et al. 1994; Carmichael et al. 1996; Gao et al. 1997; Hong et al. 1998; Kim et al. 1998). Limited measurements were simultaneously made at both the source

Corresponding author address: Dr. J. Zhang, State Key Laboratory of Estuarine and Coastal Research, East China Normal University, 3663 Zhongshan Road North, Shanghai 200062, China.
E-mail: jzhang@sklec.ecnu.edu.cn

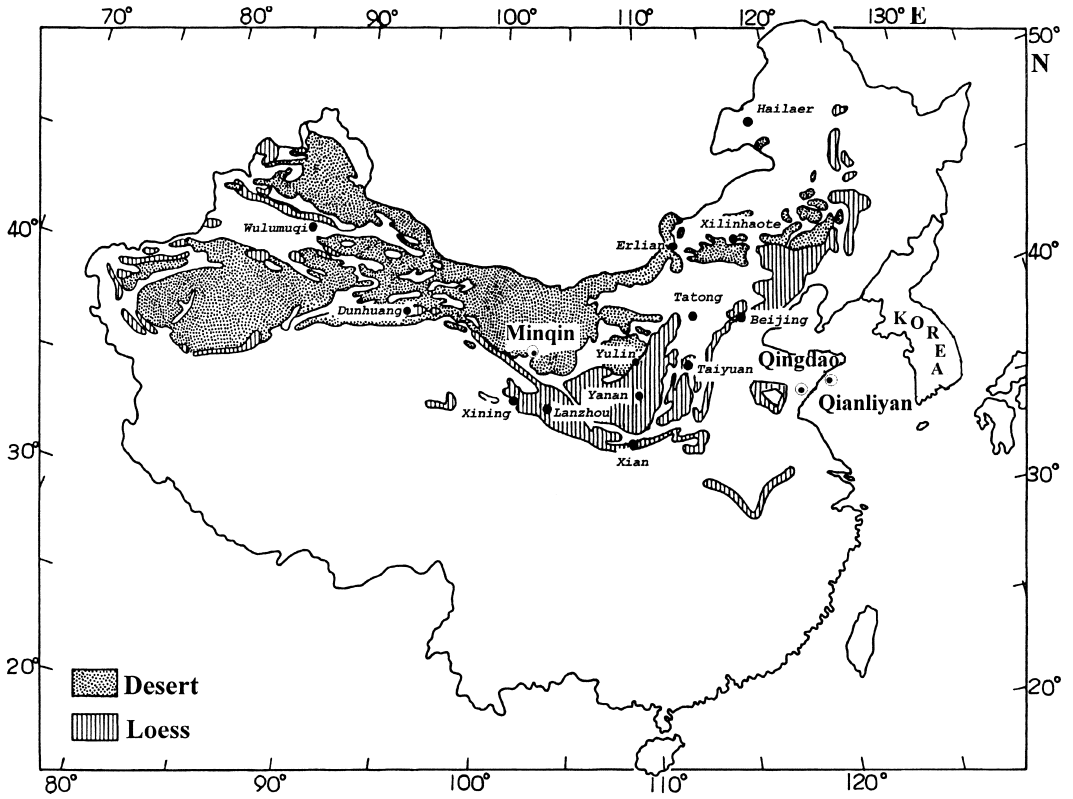

FIG. 1. Map of the study area, it shows the distribution of desert region and loess-covered area in China. The field observation sites of this study, Minqin, Qingdao, and Qianliyan, are indicated. Stations where the dust storms were recorded in springs of 1995 and 1996 in Table 4 are also shown.

region (e.g., desert) and the coastal marine recipient, that covers a considerable timescale to allow a direct comparison of aerosol composition. Hence there is no convincing aerosol data to examine the hypothesis that a coupling may exist in chemistry between dust storms in desert region and episodic high aerosol events over the coastal seas.

Here, we report the data of major components (Al, Ca, Na, Mg, K, C, and S) of aerosols collected for two years (i.e., spring and summer of 1995–96) in northwest (NW) China and the adjacent marine environment (i.e., Yellow Sea). The three sampling sites of this work (cf. Fig. 1) include a desert region [Minqin (MQ)], a coastal suburb [Qingdao (QD)], and the interior of the Yellow Sea [Qianliyan (QLY)]. The data obtained are interpreted with regards to the relationship of major components of aerosols between source and recipient, and to the assessment of chemical character of aerosols within the framework of NW China and the adjacent coastal ocean (e.g., the Yellow Sea).

2. Methods of sample collection and analysis

a. Aerosol collection

The field observation sites were selected to follow the main pathway of spring dust storms in North China (Fig. 1), that is, a desert–source region (Minqin), a coastal suburb station (Qingdao), and a marine location at Yellow Sea (Qianliyan), downwind side of the main emission sources.

1) *The Minqin site.* The aerosol samples were collected at ~10 m above ground in a plant garden of the desert region in March–May 1995 and April–June 1996. The elevation is ~1130 m. There is no habitation within a distance of 1 km. The local air pollution can be from agriculture and domestic activities (e.g., burning of biomass) in rural areas.
2) *The Qingdao site.* The aerosol samples were collected on the top of a building at ~35 m above ground and 500 m from coast in April–June 1995 and May–July 1996. The elevation is 77 m. Local air pollutants can be from traffic, domestic combustion, and anthropogenic emission from upwind urban sources.
3) *The Qianliyan site.* The aerosol samples were taken on an island of 50–60 km off the coast in March–August 1995 and May–August 1996. Sampling station is in a meteorological observatory at altitude of 75 m. There are only 10–20 habitants on the island. Local air pollution can be from the nearby fishery harbour and navigation.

The low volume pumping system was used at these sites to collect aerosol samples in Nuclepore (pore size: 0.4 μm) and Whatman GF/F (pore size: 0.7 μm) filters. Sample holders were attached to the end of clean bamboo poles (4–5 m) and the pumps were installed ~10 m downwind and/or isolated from sampling system to avoid contamination. The sampling frequency was managed on daily basis (i.e., 12–24 h). The pumping rate was 120 L min^{-1} of air. The filter holder is composed of a plastic tube with inlet diameter of 45 mm to allow laminar airflow and to minimize collision of aerosols in the sampling chamber. However, there is no wind-direction control on the pump due to the difficulty of facilities. The flow meter was calibrated before use and checked again after sampling campaigns. The sampling efficiency was estimated by the microscopy examination and theoretical calculation of particle penetration. We found giant aerosol particles (>10–15 μm) on the filters from desert region and marine stations. In our experiment, the critical particle size (d_p) is ~20 μm and the particle size of 50% efficiency is 35 μm (Friedlander 2000).

The blanks were prepared essentially the same as for the sampling procedure, but without pumping. Nuclepore filters were precleaned with HCl (1:5 v/v) followed by a thorough rinse with Milli-Q water and dried at 50°C. Whatman GF/F filters were precleaned by heating at 450°C overnight. The standard sampling method of carbonaceous aerosols is still not established and concentrations measured by different techniques need not always be comparable (cf. Countess 1990).

b. Analysis of aerosols

In the laboratory, Nuclepore filters were weighed after sample collection to estimate the concentration of aerosols (mass per unit volume of air). The samples were then digested by HNO_3-HF-$HClO_4$ in airtight Teflon bombs, and solutions were analyzed by Inductively Coupled Plasma Atomic Emission Spectrometry (ICP-AES) for Al, Ca, Na, Fe, Mn, Mg, K, V, Sr, and Zn, and by Electro-Thermal Atomic Absorption Spectrophotometry (ETAAS) for Cd, Cr, Co, Cu, Ni, and Pb. The samples collected on Whatman GF/F filters were washed by dilute HCl to remove carbonates and acid-soluble sulphur (e.g., sulphate), followed by rinse with Milli-Q water to remove extra acids. The residual aerosol carbon (RAC: organic and elemental carbon) and sulphur (RAS: acid insoluble sulphur) were determined by a LeCo-355 Carbon and Sulphur Analyzer (Zhang et al. 1997). The national soil (GSS-1), riverine (GSD-5), and marine (GSMS-1), and Canadian MESS-1 standards, were analyzed daily along with batch sample sets (Ministry of Geology and Mineral Resources 1986; Liu 1997). The precision of RAC and RAS was determined by the analysis of national standards (cf. Zhang et al. 1997). Filter blanks account for 5%–10% of low-concentration samples and are subtracted from the sample readings.

The raw datasets of aerosols were examined statistically using ''SYSTAT version 5.2'' program for cluster, cross correlation, and principal component analyzes (Zhang et al. 1999).

3. Results and discussion

In this study, about 180 sample sets were collected and analyzed, each includes one filter for inorganic species on Nuclepore and one for carbon and sulphur on Whatman GF/F. Two kinds of data are available, that is, concentration on air-volume basis ($\mu g\ m^{-3}$) and percentage of aerosol mass (%), respectively. Here, we report the data of major aerosol components (i.e., Al, Ca, Na, K, and Mg), RAC, and RAS. Concentrations of other elements will be presented elsewhere. The raw datasets of this work are available upon the formal request to the corresponding author.

a. Aerosol composition

As shown in Table 1 and Fig. 2, concentration and composition of aerosols vary over a considerable range in time and space, for example, Minqin, Qingdao, and Qianliyan. With respect to the concentrations in air-volume basis, data of aerosol mass and major components are much higher at Minqin than Qingdao and Qianliyan, levels decrease regularly from the source region to the marine recipient for crust-dominated components (e.g., Al). Species from anthropogenic emission (e.g., RAC and RAS) have higher concentrations at the coastal suburb station than at the desert (i.e., Minqin) at upwind-side and downwind marine station (Qianliyan; Fig. 2). Sea salt component (i.e., Na) may show higher levels at the coast than at inland stations. Differences in air-volume-based data appear between the 1995 and 1996 campaigns; concentrations can be lower in 1996 than 1995 for Minqin and Qianliyan; samples from 1995 may have higher variations. At Qingdao, the observed species have lower concentrations in 1995 than 1996, the 1996 samples have also an increase in concentration range (Fig. 2). When comparing the data of aerosol mass in percentage (%), different features are found (Fig. 2). Aluminum again shows a higher concentration at Minqin than coastal stations at the downwind side (i.e., Qingdao and Qianliyan), the difference between 1995 and 1996 is minimized (Fig. 2). The major sea salt component (i.e., Na) increases from the desert region to the coastal atmosphere; concentrations (%) of Na can be five- to tenfold higher at Qianliyan than at Minqin (Fig. 2). Calcium and K have higher values, whereas Mg has lower concentrations in percentage at Qingdao compared to both Minqin and Qianliyan (Table 1 and Fig. 2).

By normalizing element concentration to the atmospheric end-member index, that is, the reference ele-

TABLE 1. Composition of aerosols from northwest China desert region and Yellow Sea. The datasets show (a) air-volume-based concentration (μg m^3) and (b) percentage (%) of aerosol mass.

Composition	Concentration	Minqin		Qingdao		Qianliyan	
		1995	1996	1995	1996	1995	1996
(a) Air-volume-based concentration (μg m^{-3})							
Aerosol	Range	20–2060	14–378	16–180	6.5–327	4.1–57.0	3.3–35.5
	Geometric mean	90.8	98.6	60.2	33.0	18.4	12.1
	Average	187	131	68.8	49.2	23.0	15.0
	50th percentile	1040	196	98.0	167	30.6	19.4
Al	Range	1.39–153	0.72–28.7	0.82–9.32	0.16–23.1	0.11–2.28	0.03–1.87
	Geometric mean	6.35	6.25	2.42	1.27	0.57	0.25
	Average	13.6	8.79	2.93	2.53	0.83	0.45
	50th percentile	77.2	14.7	5.07	11.6	1.19	0.95
Ca	Range	1.08–113	0.74–27.8	0.92–9.72	0.23–15.2	0.05–1.79	0.07–1.76
	Geometric mean	5.70	6.21	3.04	1.35	0.55	0.32
	Average	11.4	8.41	3.59	2.25	0.74	0.43
	50th percentile	57.0	14.3	5.32	7.72	0.92	0.92
Na	Range	0.28–41.8	0.14–6.39	0.25–4.76	0.05–5.58	0.17–5.41	0.04–1.99
	Geometric mean	1.37	1.24	1.29	0.67	0.89	0.39
	Average	3.22	1.80	1.71	0.92	1.29	0.55
	50th percentile	21.0	3.27	2.51	2.82	2.79	1.02
Mg	Range	0.46–46.7	0.24–9.63	0.22–2.18	0.08–5.52	0.03–1.04	0.04–0.49
	Geometric mean	2.14	2.07	0.78	0.36	0.28	0.16
	Average	4.40	2.88	0.89	0.61	0.36	0.19
	50th percentile	23.6	4.94	1.20	2.80	0.54	0.27
K	Range	0.45–51.7	0.26–8.39	0.29–4.51	0.10–7.97	0.07–1.14	0.02–0.92
	Geometric mean	1.99	2.14	1.07	0.65	0.33	0.18
	Average	4.42	2.92	1.34	1.17	0.42	0.30
	50th percentile	26.1	4.32	2.40	4.04	0.60	0.47
RAC	Range	1.52–23.8	1.40–11.3	3.86–18.4	0.65–30.4	0.29–13.2	0.45–6.56
	Geometric mean	3.12	3.64	8.15	3.59	2.08	1.59
	Average	4.27	4.19	8.88	5.08	3.10	2.12
	50th percentile	12.7	6.35	11.1	15.5	6.75	3.51
RAS	Range	0.01–1.52	0.02–1.13	0.12–0.84	0.02–1.08	0.01–0.78	0.02–0.30
	Geometric mean	0.12	0.13	0.24	0.11	0.06	0.09
	Average	0.17	0.22	0.27	0.16	0.11	0.11
	50th percentile	0.77	0.58	0.48	0.55	0.39	0.16
(b) Percentage concentration (%) of major species in aerosols							
Al	Range	5.43–9.31	4.93–7.96	1.85–6.36	1.23–7.08	0.96–6.79	0.42–7.06
	Geometric mean	6.99	6.34	4.02	3.84	3.12	2.08
	Average	7.04	6.40	4.23	4.21	3.71	2.55
	50th percentile	7.37	6.45	4.11	4.16	3.88	3.74
Ca	Range	4.74–8.39	4.52–8.40	2.33–10.7	2.21–24.5	1.33–15.7	1.03–7.08
	Geometric mean	6.28	6.30	5.06	4.09	3.02	2.61
	Average	6.34	6.36	5.42	4.74	3.47	2.89
	50th percentile	6.57	6.46	6.52	13.4	8.52	4.06

TABLE 1. (*Continued*)

Composition	Concentration	Minqin		Qingdao		Qianliyan	
		1995	1996	1995	1996	1995	1996
Na	Range	1.00–2.39	0.95–1.82	0.53–8.49	0.46–9.62	1.23–15.6	0.38–29.4
	Geometric mean	1.51	1.26	2.14	2.04	4.87	3.24
	Average	1.55	1.28	2.71	2.66	6.03	6.12
	50th percentile	1.69	1.38	4.51	5.04	8.42	14.9
Mg	Range	1.93–3.45	1.63–2.55	0.49–2.28	0.59–2.31	0.68–2.72	0.51–5.92
	Geometric mean	2.36	2.10	1.30	1.10	1.45	1.33
	Average	2.38	2.12	1.38	1.16	1.56	1.63
	50th percentile	2.69	2.09	1.39	1.45	1.70	3.22
K	Range	1.54–2.88	1.84–2.33	0.68–2.84	0.74–7.66	0.88–2.80	0.21–4.10
	Geometric mean	2.19	2.17	1.78	1.96	1.71	1.48
	Average	2.21	2.17	1.86	2.21	1.80	1.74
	50th percentile	2.21	2.09	1.76	4.20	1.84	2.16

ments of crustal material (e.g., Al) and sea salt (e.g., Na), the chemical fingerprint of observed air mass emerges. Within the framework of the observation in the present study, three important sources of chemical elements (end-member) to the air mass sampled can be identified:

1) low-temperature weathering products of crust, which are characterized by the predominance of mineral particles;
2) a variety of local materials such as high-temperature anthropogenic emission, the percentile of which increases along the trajectory of air mass from remote to urban areas; and
3) marine aerosols, which are produced by the processes of sea salt generation at sea surface and in lower atmosphere.

The contribution of principal sources of elements to aerosols can be estimated by using enrichment factors (EF), with Al and Na as reference index of crustal and sea salt components, respectively (cf. Zhang et al. 1999; Chester et al. 2000). The EFc—that is, noncrustal enrichment—is calculated by the equation

$$\mathrm{EFc} = \frac{(\mathrm{Cx/Al})\mathrm{aerosol}}{(\mathrm{Cx/Al})\mathrm{crust}}, \tag{1}$$

where (Cx/Al)aerosol represents the concentration ratio of element x (Cx) to Al in aerosol, and (Cx/Al)crust stands for the corresponding element (Cx) to Al ratio in crust materials. Similarly, the contribution of non–sea salt (EFs) can be estimated by the equation

$$\mathrm{EFs} = \frac{(\mathrm{Cx/Na})\mathrm{aerosol}}{(\mathrm{Cx/Na})\mathrm{sea\ salt}}, \tag{2}$$

in which (Cx/Na)aerosol is the element x (Cx)-to-Na ratio in aerosol, and (Cx/Na)sea salt the element x (Cx)-to-Na ratio in sea salt, respectively. In this study, we use average seawater and soil compositions as references, and data of EFc and EFs are given in Table 2. By convention, the EF ≤ 10 is considered to show that metal in aerosols has a significant crust (EFc) and/or marine (EFs) contribution, and hence termed the nonenriched element. The EF > 10 indicates that element has an important proportion of noncrustal and/or nonmarine sources and hence termed the enriched element (Chester et al. 2000). When the aerosol compositions are presented in this manner, a number of features appears and can be identified from Table 2.

1) At Minqin, EFc < 5 is found for all inorganic species of interest, which is true for samples from both 1995 and 1996 campaigns. Moreover, none of species (Ca, Mg, and K) has EFs < 10 in Table 2. This suggests that element compositions have a predominant source of crustal materials, and none of the species at Minqin has a considerable input of marine aerosols. Even Na has a close

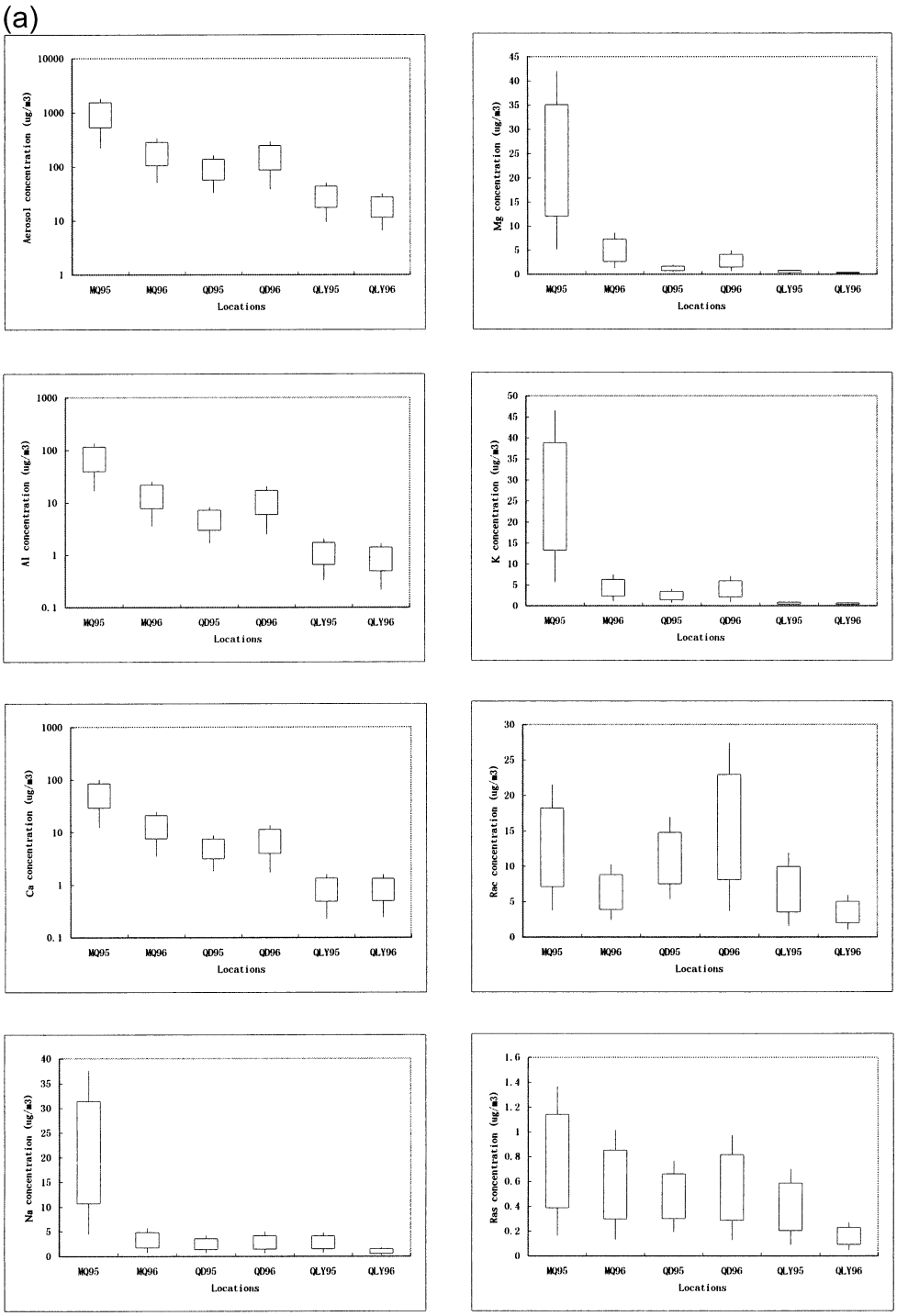

FIG. 2. Aerosol compositions of MQ, QD, and QLY in 1995 and 1996 observations, with (a) concentrations in air-volume basis (μg m^{-3}) and (b) concentrations in percentage of aerosol mass (%). In the figure, the distribution of aerosol mass and major components are shown as the 10th, 25th, 75th, and 90th percentiles. The 50th percentile is given in Table 1 to compare with the arithmetic average and geometric mean.

relation with Al at Minqin, a characteristic of remote inland station that represents the source of cruatal aerosols (Table 2).

2) At Qingdao, the average EFc of Ca (2.86/3.37), Mg (1.74/1.95), Na (1.48/1.48), and K (1.27/1.47) indicate that these elements have a dominant contribution of crustal materials, though the maximal EFc of Ca may reach 28.3 in 1996 (Table 2). Magnesium

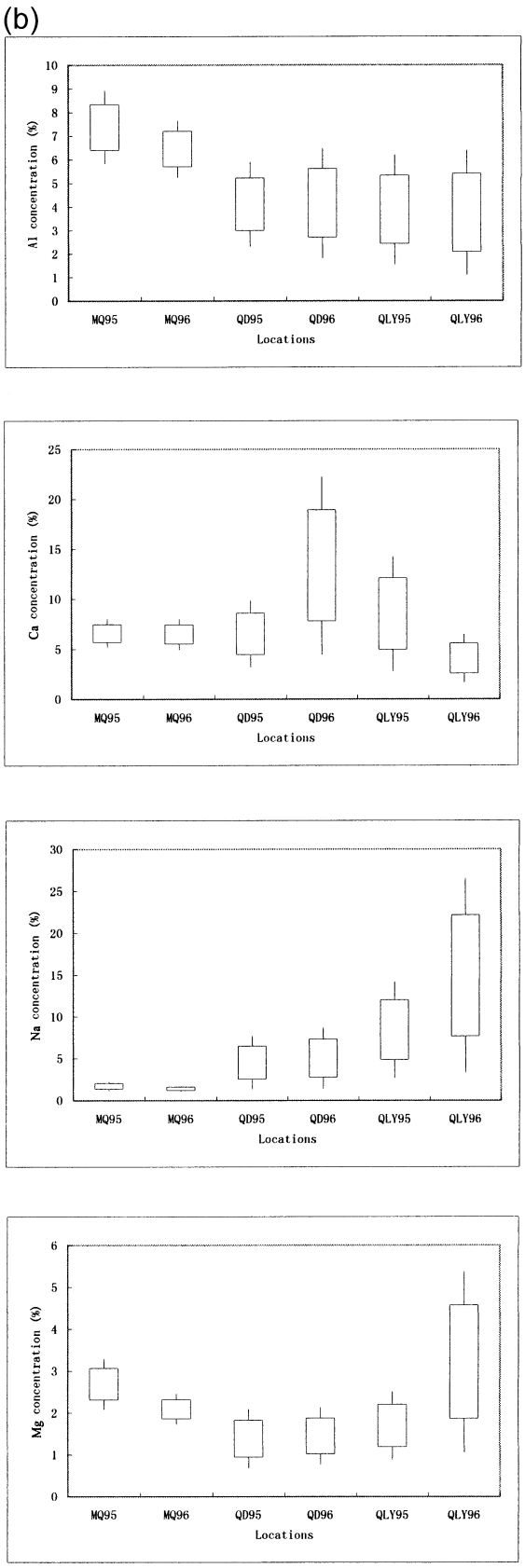

FIG. 2. (*Continued*)

at Qingdao has nonenriched character with respect to sea salt, because EFs of Mg is 1.75–11.8, whereas sea salt input is minimized for K (EFs = 4.11–167) and Ca (EFs = 11.3–224) (Table 2). This suggests that a mixture of different air masses (e.g., local particles and sea salt) feeds aerosol composition at Qingdao to various extents, depending upon the element of interest.

3) At Qianliyan, the EFc values indicate that Ca (2.44/3.37) and K (1.56/2.04) have a dominant input of crustal materials. Sodium has a dominant noncrustal character with EFc value up to 101. At this station, Mg shows a feature of mixed inputs of crustal and marine aerosols, because its EFc and EFs values are comparable (Table 2). Calcium and K illustrate, however, a strong anomaly when normalized against Na.
4) When normalized to crustal index (i.e., Al), RAC and RAS show quite different enrichment features in this study (Table 2). The EFc for RAC is lower at Minqin (5.26/6.36) relative to Qingdao (37.0/31.4) and Qianliyan (32.0/52.6), indicating a remote character of aerosols. The EFc of RAC increases in coastal marine atmosphere, presumably owing to an enhanced anthropogenic emission (e.g., burning of fossil fuels) in China (Parungo et al. 1994; Kim et al. 1998).

Aerosol composition of the source region (e.g., Minqin) is considerably stable, the geometric mean of major components differ by <10%–20% when data are expressed as percentage of aerosol mass, and hence element ratios (Table 2). The crustal ratios of major species to Al can be 20% higher on average for desert aerosols, than loess.

The comparison between these stations indicates that aerosols of Minqin represents a typical crustal aerosol assembly, Qianliyan shows a character of aerosols composed of a considerable amount of marine aerosols. The aerosol composition at Qingdao has a feature of neither crustal nor marine end members, but rather, a mixture of air masses with fingerprints of local emission, taking into account the high levels of RAC and RAS (Table 2).

b. Element relationship and comparison with previous data

There are several publications from North Pacific and eastern Asia in literature that can be compared with this study. Gao et al. (1992, 1997) reported aerosol data at two urban–suburban stations (i.e., Mallipo and Qingdao) around the Yellow Sea, with 0.6–6.7 μg m^{-3} for Al and 0.5–11 μg m^{-3} for Na at Mallipo in 1989, and 2.5 $\pm$ 2.2 μg m^{-3} for Al at Qingdao in 1992. These values are generally comparable to our results from Qingdao, but higher when compared to Qianliyan. It should be kept in mind that uncertainties, owing to the different sampling–analytical methods in this study (low-volume

TABLE 2. Enrichment factors of major aerosol components at Minqin, Qingdao, and Qianliyan. It shows the (a) EFc and (b) EFs values for whole datasets in this study.

Components	EF	Minqin		Qingdao		Qianliyan	
		1995	1996	1995	1996	1995	1996
		(a) EFc for aerosol components					
Ca	Range	1.90–3.05	2.02–3.23	1.48–7.38	1.23–28.3	0.75–7.07	1.49–12.5
	Geometric mean	2.38	2.64	3.37	2.86	2.44	3.37
	Average	2.40	2.66	3.66	3.68	2.68	3.98
Mg	Range	1.83–2.51	1.77–2.51	1.14–4.78	0.88–5.02	0.90–14.9	1.29–37.9
	Geometric mean	2.03	2.00	1.95	1.74	2.78	3.88
	Average	2.04	2.01	2.13	1.94	3.54	6.54
Na	Range	0.39–1.11	0.39–0.73	0.58–8.12	0.53–9.97	0.62–45.2	0.56–101
	Geometric mean	0.59	0.54	1.48	1.48	4.18	4.35
	Average	0.61	0.55	1.99	2.31	7.22	13.54
K	Range	0.76–1.02	0.83–1.27	0.84–2.35	0.70–4.92	0.37–6.41	0.37–12.3
	Geometric mean	0.90	0.98	1.27	1.47	1.56	2.04
	Average	0.90	0.98	1.31	1.66	1.80	2.47
RAC	Range	1.06–34.2	1.62–101	13.0–175	7.38–119	11.5–85.8	10.2–143
	Geometric mean	5.26	6.36	37.0	31.4	32.0	52.6
	Average	5.20	11.2	45.4	37.8	38.6	65.8
		(b) EFs for aerosol components					
Ca	Range	71.0–167	85.3–196	13.9–146	11.3–224	2.78–89.1	3.16–135
	Geometric mean	109.1	131.5	61.8	52.4	15.8	21.0
	Average	111.8	134.6	73.8	69.7	20.5	35.1
Mg	Range	6.92–18.0	10.0–20.5	2.07–9.31	1.75–11.8	1.27–8.82	1.13–21.1
	Geometric mean	13.2	14.1	5.08	4.50	2.56	3.43
	Average	13.5	14.4	5.61	5.26	2.85	4.36
K	Range	18.7–68.5	35.8–65.9	4.11–65.9	4.76–167	1.60–43.6	1.42–156
	Geometric mean	41.7	49.3	23.6	27.2	10.2	12.9
	Average	42.8	49.9	29.2	37.3	12.9	27.7

TABLE 3. Multivariable correlation matrices of aerosol composition from Minqin, Qingdao, and Qianliyan.

Species	Al	Ca	K	Mg	Na	RAC	RAS
				Minqin			
Al	1.00						
Ca	0.43	1.00					
K	0.74	0.29	1.00				
Mg	0.82	0.54	0.65	1.00			
Na	0.39	0.25	0.21	0.44	1.00		
RAC	−0.35	−0.28	−0.29	−0.29	−0.29	1.00	
RAS	−0.35	−0.23	−0.25	−0.28	−0.27	0.90	1.00
				Qingdao			
Al	1.00						
Ca	0.03	1.00					
K	0.31	−0.07	1.00				
Mg	0.26	0.39	−0.09	1.00			
Na	−0.16	0.12	−0.08	0.66	1.00		
RAC	−0.01	0.06	−0.08	0.08	−0.03	1.00	
RAS	−0.23	−0.11	−0.21	−0.06	0.08	0.51	1.00
				Qianliyan			
Al	1.00						
Ca	0.83	1.00					
K	0.75	0.72	1.00				
Mg	0.21	0.59	0.22	1.00			
Na	−0.17	0.22	−0.06	0.88	1.00		
RAC	−0.30	−0.16	−0.16	0.13	0.21	1.00	
RAS	−0.33	−0.20	−0.22	0.16	0.29	0.85	1.00

pump with precleaned Nuclepore filter) and Gao et al. (high-volume pump with Whatman 41 sheet), remain unknown. Carmichael et al. (1996) and Kim et al. (1998) reported water-soluble concentration for Na (1–8 μg m^{-3}) and Ca (0.1–3.0 μg m^{-3}) from aerosols at Cheju Island. These data are higher in average compared to Qianliyan, but lower for Ca when compared to Qingdao. Most likely, part of the aerosol Ca and Na is not soluble and hence not covered by the previous studies (Carmichael et al. 1996; Kim et al. 1998). Concentrations of Na^+ (0.3–9.2 μg m^{-3}), Mg^{2+} (0.0–2.2 μg m^{-3}), Ca^{2+} (0.1–8.5 μg m^{-3}), and K^+ (0.0–2.4 μg m^{-3}) reported by Chen et al. (1997) from Cheju Island in 1993–95, are ranked at intermediate positions between datasets of Qianliyan and Qingdao. Again, none of previous studies allows, a source and recipient comparison of aerosol compositions. Elemental and organic carbon (EC + OC) reported by Kim et al. (1998) are 0.27 ± 0.05 μg m^{-3} and 3.74 ± 0.39 μg m^{-3}, respectively, with the EC + OC value lower than that observed from Qingdao (6.98 ± 4.38 μg m^{-3}) but similar to Qianliyan (4.54 ± 2.17 μg m^{-3}). The elevated RAC values from Qingdao is probably because that this site is located downwind of strong emission sources in North China. The difference in aerosol compositions between Cheju and Qingdao–Qianliyan arises in part from the sampling strategy that data from Cheju are for $PM_{2.5}$ (which is kinetic aerosol size $<$ 2.5 μm in diameter; Kim et al. 1998), rather than the total concentration as for Qingdao and Qianliyan. A large amount of RAC was found to exist in the isokinetic size $>$2.5 μm in this region (Parungo et al. 1994).

c. Data processing by statistics

The results of statistics are given in Table 3 for cross correlations and Figs. 3–4 for cluster and principal component managements, respectively.

With respect to cluster analysis, data from Minqin, Qingdao, and Qianliyan illustrate different features. At Minqin, two groups are identified, the first group includes Al, Ca, K, Mg, and Na, confirming the dominance of crustal materials over the aerosol composition (Fig. 3). The correlation matrix shows the positive relationship among these elements (Table 3). Aluminium concentrations and total aerosol mass are directly correlated ($\gamma^2 = 0.998$, $n = 58$) at Minqin, such a relationship deteriorates at coastal suburb station further down wind (e.g., Qingdao). The second group contains RAC and RAS, which is well separated from group-one elements, suggesting that RAC and RAS come from a different source, presumably organic materials (e.g., organic debris) and anthropogenic emission (e.g., burning of biomass; Fig. 3). A statistically significant relationship between RAC and RAS has been found, both species are negatively related with crust dominated elements in correlation matrix (Table 3).

At Qingdao, three groups can be identified. Aluminium and K are closely correlated, suggesting their dominant source of crustal materials. The second group contains Na, Mg, and Ca. The RAC and RAS, indicating different sources/processes involved, form the third group. This is in agreement with a negative correlation between RAC–RAS and elements of two other groups. Sea salt is probably a major source of Na and Mg at

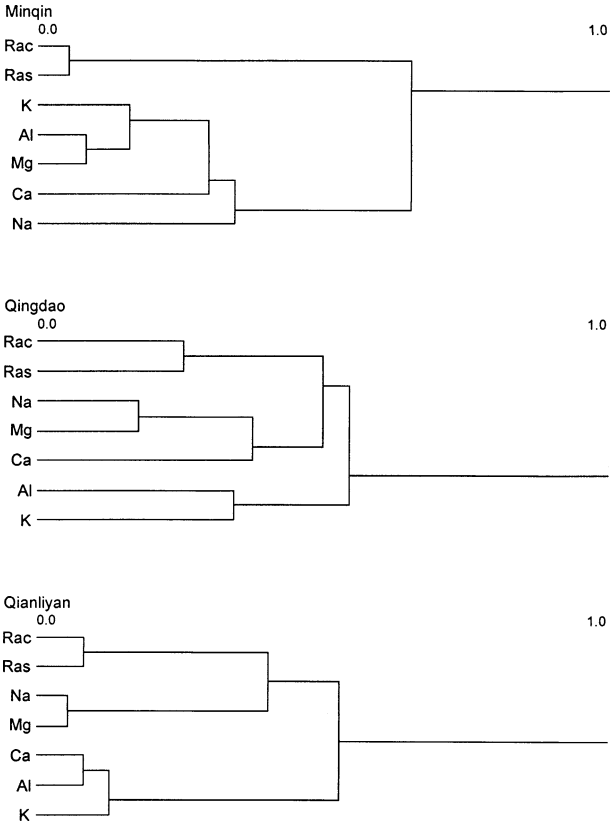

FIG. 3. Cluster analysis for aerosol data from MQ, QD, and QLY. The Pearson correlation coefficient and average link method are used. The figure shows the tree diagram of correlation distance among major components in this study.

Qingdao, because Na shows a negative relationship with Al (Table 3).

At Qianliyan, Al, Ca, and K are closely linked and form one group. The correlation matrix shows the positive relationship among Al, Ca, and K (Table 3 and Fig. 3). Sodium and Mg form another group, which is then connected with group-three species (RAC and RAS). RAC and RAS illustrate a positive relationship (Table 3), suggesting an anthropogenic source for these components.

The principal component analysis provides further information relevant to the contribution of various source materials into the air. The four factors (F1 to F4) account for 85%–95% of total information. At Minqin, RAC and RAS have important negative loading on F2 factor, while Al, Ca, K, Mg, and Na show the significant loading on factor F1 (Fig. 4). This implies that F1 indicates the crustal input of aerosol components, F2 underlies the contribution from anthropogenic emission. Similarly, RAC and RAS illustrate important loading on F2 at Qingdao, and Al and K have higher fractions on factor F3. Magnesium and Na have an important loading on F1, and Ca shows a higher loading on factor F4 (Fig. 4). The comparison of data from these two stations indicates that source materials are diverse at Qingdao and vary considerably depending on the element of interest. For example, F1 represents the sea salt input, F2 represents the anthropogenic emission, F4 may show a local source, while F3 stands for crustal materials (Fig. 4). Finally, at Qianliyan, RAC and RAS have dominant loading on F3, indicating their common source of anthropogenic emission. Aluminium, K, and Ca show higher loading on F1 and F4 relative to F2, suggesting the input from crustal materials. A significant loading of Na and Mg on F2 provides evidence of sea salt contribution to the aerosols at marine station (Fig. 4). It is interesting to note from cluster statistics that Ca is weakly associated with Na and Mg at Qingdao, but has a close relationship with Al and K at the offshore region (i.e., Qianliyan). While at Qianliyan the strong linkage with Al indicates that Ca is most likely of crustal origin, the principal component analysis shows that Ca at Qingdao is from a different but regional emission source as compared to Na and Mg.

In summary, the statistical data processing confirms that:

1) Al, Ca, K, Mg, and Na in aerosols are dominated by the crustal materials at desert region;
2) Al still has a dominant terrigenous source of crustal materials in coastal areas, that can be local soil particles and/or fly-ash from combustion. Sodium becomes dominated by the sea salt contribution in coastal areas, with Ca, K, and Mg at intermediate position, and
3) in any of the cases, RAC and RAS have a common but distinctive source that can be either from organic detritus (e.g., tree/herb debris) or anthropogenic emission (e.g., black carbon), or both.

d. Character of aerosol composition over the Yellow Sea

The averaged seasonal mean wind field data for 2 yr (1995 and 1996) show the difference between spring and summer. The northwesterly winds dominate at both near-surface (i.e., 1000 and 850 hPa) and 3000 m msl (e.g., 700 or 500 hPa) in northern China in spring (Fig. 5).

Data of wind field show a similar pattern between 1995 and 1996, but some fine structures can be identified. In spring, the seasonally northwest high is stronger in 1995 than in 1996, which is reflected by an increased dust storm records at ground level for most stations (Table 4). At the 500-hPa level, a very strong and dominant eastward airflow could carry the aerosols toward the North Pacific Ocean once the soil particles are initiated by the cyclones at near-surface. In the southern part of country and adjacent coastal ocean, the eastward and westward low-pressure systems converge, inducing a northward airflow at near-surface level. This is, however, not found at 500 hPa. In summer, wind field data show a decrease of westerly wind and the enhancement of easterly and southerly winds over the China Sea for both 1995 and 1996.

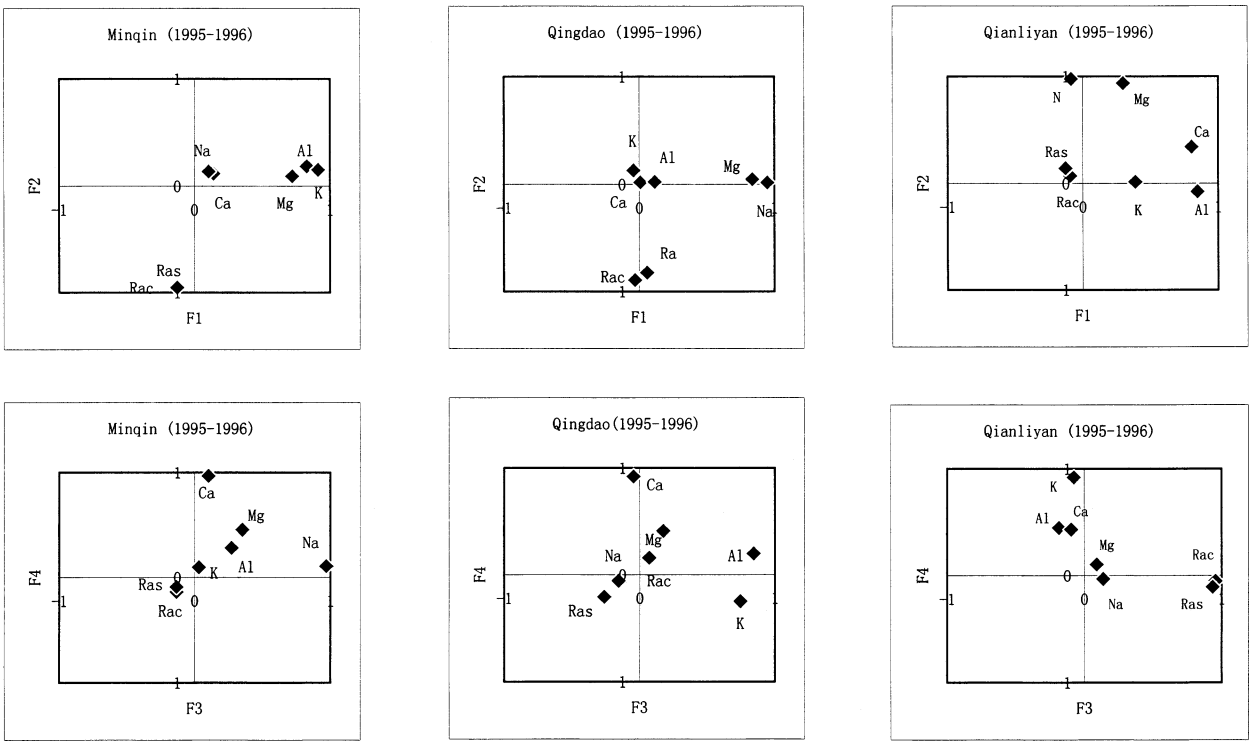

FIG. 4. Results of principal factor analysis of aerosol data from MQ, QD, and QLY. Four components (F1–F4) are identified which account for 85%–95% of the total variability.

The southwest monsoon is also increased, followed by a better developed cyclone at low latitude, such a wind field induces a decrease of soil dust transport by westerlies at near ground level and an increase in humid air mass carried by southwest (Indian Ocean) and southeast (Pacific Ocean) monsoons. At the 500-hPa level, the influence of westerlies is much weaker in summer than in spring, the southwest and southeast monsoons occupy most of the country (Fig. 5).

From airmass back-trajectory data, it is very clear that episodic increase in amount of aerosols and percentage concentration of lithogenic elements (e.g., Al) in marine atmosphere is related to the dust storms in the desert region in spring (cf. Chung 1992; Chen et al. 1997; Zhang and Iwasaka 1999). A certain amount of Al can be injected into atmosphere by anthropogenic processes, such as the combustion of fossil fuels (e.g., coal-ash) and local soil dust (Gao et al. 1997; Zhang and Iwasaka 1999). The real contribution of crustal aerosols to the coastal ocean atmosphere is probably lower than what is estimated from the air-volume-based concentrations for aluminium because of the lack of percentage data (%) in aerosols (Gao et al. 1997). The particle size tends to change after the mineral aerosols are initiated from the source region and transported eastward. It can be expected that percentage concentration of Al would increase with smaller particle size of crustal aerosols along the trajectory over coastal ocean. For a typical clay composition, Al level can be as high as 10%–20%. Such a size effect should be minimized when the dust storms pass through over coastal ocean in spring, owing to strong influence of mineral aerosols and rapid meteorological processes in combination.

At Qingdao, aerosol Al in percentage has a poor relationship with total aerosol mass, which is true for both 1995 and 1996 samples. There is no simple relationship

TABLE 4. Recorded dust storm events from selected northern China desert and loess regions in the springs of 1995–96. The spring season is defined as Mar–May. Note that dust events are much more serious in the desert region than loess-covered area at the downwind side. The geographic location of these stations is indicated in Fig. 1.

Station	1995	1996	Landscape
Wulumuqi	0	1	Desert
Dunhuang	16	30	Desert
Minqin	25	19	Desert
Xining	1	2	Loess
Lanzhou	12	7	Loess
Xi'an	4	0	Loess
Yan'an	13	7	Loess
Yulin	3	2	Desert–loess
Taiyuan	1	2	Loess
Datong	4	2	Loess
Erlian	5	3	Desert
Hailaer	3	0	Desert
Xilinhaote	5	1	Desert
Beijing	4	6	City

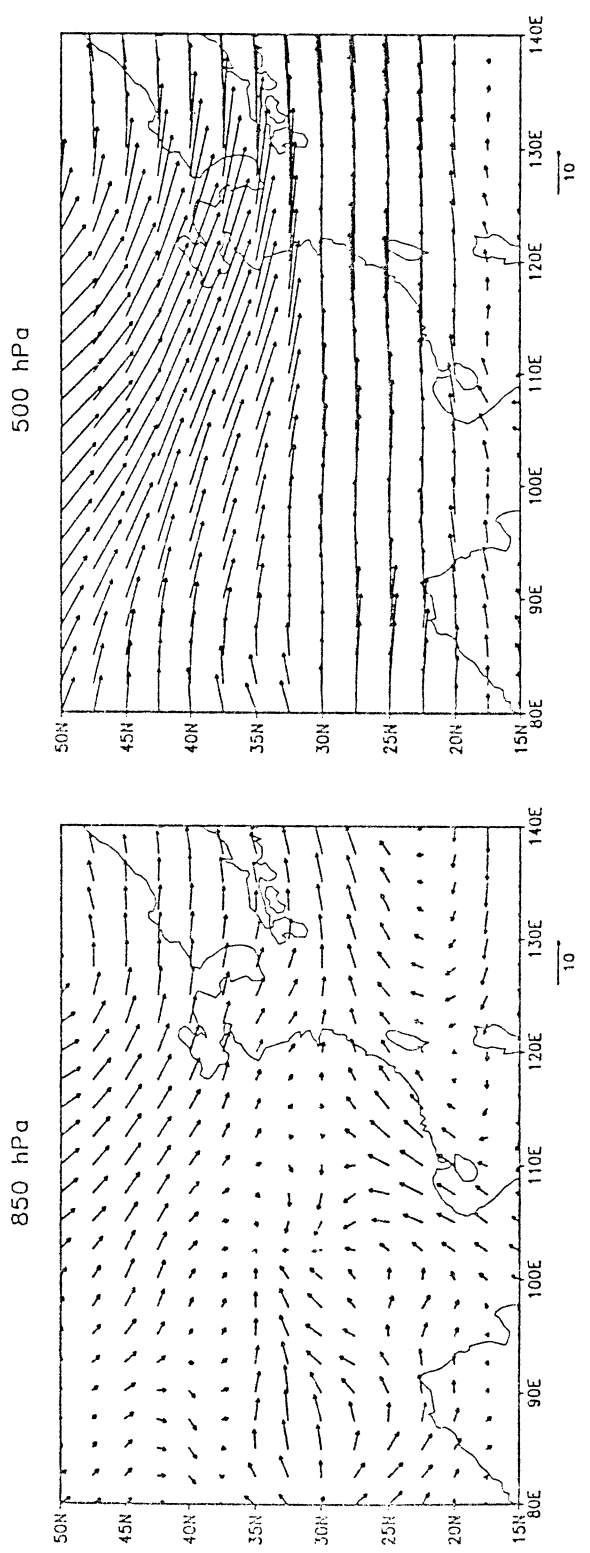

FIG. 5. The 850- and 500-hPa seasonally (spring: upper panels, summer: lower panels) mean wind fields for China. The main features of wind field data are similar between 1995 and 1996, hence data of 1995 are plotted here. Data are from National Oceanic and Atmospheric Administration–Cooperative Institute for Research in the Atmosphere's Climate Diagnostic Center, Boulder, Colorado.

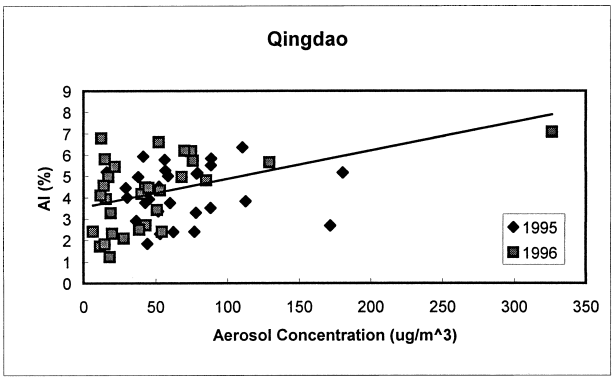

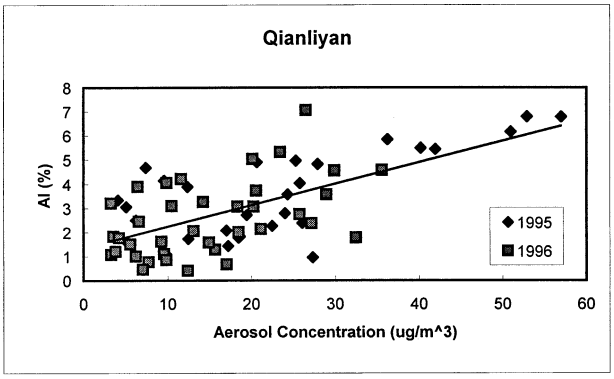

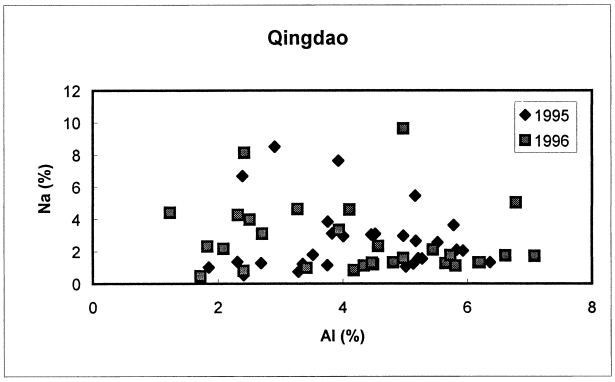

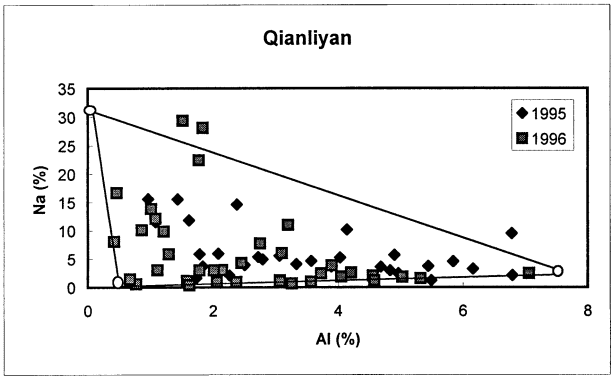

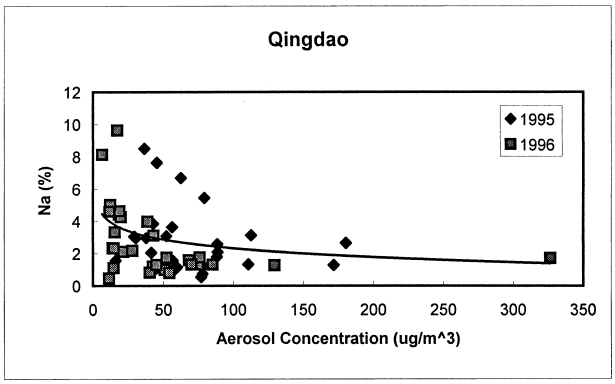

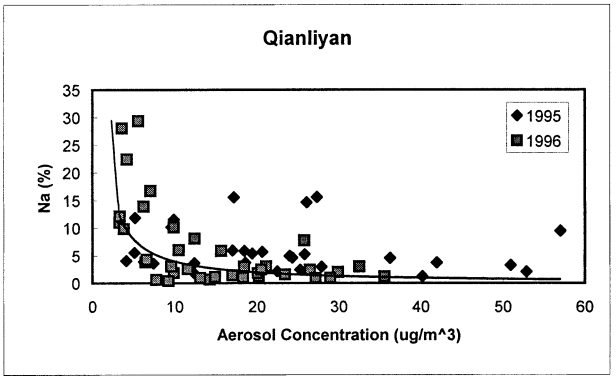

FIG. 6. Relationship between major inorganic components of aerosol samples at Qingdao, which shows the plots among Al, Na, and aerosol concentrations, indicating a mixing pattern of local source, long-distance dust transport, and sea salt. The figure shows also the simulation by least square (line) and multinomial (curve) methods with a correlation coefficient $\gamma^2 = 0.11$ between Al and aerosol levels.

FIG. 7. Relationship between major inorganic components of aerosol samples at Qianliyan, which shows the plots among Al, Na, and aerosol concentrations, indicating a mixing pattern of regional source, long-distance dust transport, and sea salt. The figure shows also the simulation by least square (line) and multinomial (curve) methods. A linear relationship between Al and aerosol level can be seen ($\gamma^2 = 0.42$), while Na falls hyperbolically with higher aerosol concentrations. The triangle of the Na–Al diagram suggests that aerosol samples at this station be products of mixture between three end members in various proportions.

between Al and Na, due to different source materials involved at coastal suburb area (Fig. 6). Sodium tends to decrease with higher aerosol concentrations at Qingdao, although data are scattered (Fig. 6). At Qianliyan, Al in percentage increases with higher concentrations of aerosol, indicating that crustal component is increased when the aerosol level is high (i.e., cold front; Fig. 7). Sodium in percentage can be significantly reduced by dust storms, hence the sea salt contribution (Fig. 7). Qianliyan samples occupy a triangular region in the diagram of Na (%) versus Al (%). The compositions of aerosol at the three corners of this triangle correspond to the aerosols of crust material (Minqin: Al, 7.5% and Na, 1.5%), to sea salt (Al, 0% and Na, 30.8%), and to probably a regional source (Al, 0.5%

TABLE 5. Parameters used in simulation of aerosol components at the Yellow Sea. The details of parameter definition are given by Eq. (4) in the text.

Parameter	Local source (X_1)	Dust (X_2)	Sea salt (X_3)
Aerosol level (Y_1)	$a_{11} = 1.0$	$a_{12} = 1.0$	$a_{13} = 1.0$
Al (Y_2)	$a_{21} = 0.5$	$a_{22} = 7.5$	$a_{23} = 0$
Na (Y_3)	$a_{31} = 0.2$	$a_{32} = 1.5$	$a_{33} = 30.8$

and Na, 0%), respectively (Fig. 7). In Fig. 7, mixing these end-members in various proportions forms the sample points within the triangle. While it is possible that other aerosol types with compositions lying within the triangle also contribute, this is unlikely since the source regions for such aerosols have not been identified. A similar relationship among Al, Na, and with aerosol mass cannot be established with the available dataset from Qingdao, although at higher aerosol concentrations the percentage concentration of Na trends to decrease too (Fig. 6). Moreover, a regular change in aerosol composition was found at Qianliyan, where Na concentration in aerosols ranges from $<1.0\%$ to 20%–25% within a typical period of 1 week to 10 days, corresponding to the episodic dust storm events.

To test the hypothesis of coupling of aerosol compositions between source region (e.g., Minqin) and marine recipient (e.g., Yellow Sea), we normalized Al concentration from Qianliyan [Al (QLY)] to the average Al level of Minqin [Al (MQ)] and compared the data to meteorological information. An increase in [Al (QLY)]/[Al (MQ)] may suggest a higher proportion of dust-materials in marine atmosphere, while fall in [Al (QLY)]/[Al (MQ)] indicates a pronounced contribution from sea salt and/or local source in atmosphere. The Al to end-member ratio [i.e., Al (QLY)/Al (MQ)] at Qianliyan increases up to 0.9–1.0 when the dust storms pass through over the Yellow Sea, and falls to 0.1–0.2 when the cold fronts expire (Fig. 8). Again, low EFc and high EFs values appear exclusively when cold fronts pass through over the Qianliyan. In the meantime, sea salt (i.e., Na) and local emission (e.g., RAC) are considerably decreased as compared to nonfront periods (Fig. 8). This indicates a rapid atmospheric reloading and wash-out/removal over the Yellow Sea. While atmospheric reloading of sea salt aerosol is sustained continuously by the underlying ocean at surface, the removal/scavenging mechanisms of sea salt aerosols is not straightforward, either due to removal by precipitation or dilution in proportion by crustal materials (e.g., dust storm) and anthropogenic emission (e.g., RAC; Fig. 8). Indeed, the expiration of dust storms in Fig. 8 corresponds to an increase in sea salt concentration in summer and a considerable level of RAC in winter. The scavenging of aerosols via wet-deposition was examined by the comparison between rainfall and aerosol levels in time and space (Zhang et al. 1999). This phenomenon was poorly documented, however, in literature because the percentage concentration of individual components was omitted in previous studies, or data are incomplete (cf. Gao et al. 1997).

e. A simple mixing model

Assuming that the aerosols observed over the Yellow Sea are composed of m components supplied via n different sources/pathways, the contribution of individual sources/pathways to the aerosol composition at marine station can be estimated by matrix arithmetic:

$$\begin{bmatrix} a_{11} & a_{12} & \cdots & a_{1m} \\ a_{21} & \cdots & & \\ \vdots & & & \\ a_{n1} & a_{n2} & \cdots & a_{nm} \end{bmatrix} \begin{bmatrix} X_1 \\ X_2 \\ \vdots \\ X_m \end{bmatrix} = \begin{bmatrix} Y_1 \\ Y_2 \\ \vdots \\ Y_n \end{bmatrix}, \tag{3}$$

where (a_{ij}) represents the percentage concentration of the jth component in the ith source material (X_i), Y_i accounts for the ith element concentration (%) in marine atmosphere (e.g., Yellow Sea). The weight factor (a_{ij} in %) of various source contributions to the observed aerosol composition (%) can be solved by statistics (e.g., least-squares method) when $m \neq n$ (Haswell 1992). In the case of $m = n$, a definite solution can be obtained. From previously published results and precedent discussion (cf. Fig. 7), three important sources can be identified for the aerosol samples in marine atmosphere over the Yellow Sea, including long-distance transport of crustal materials with chemical composition similar to loess and/or desert soils, sea salts having stoichiometric element ratio identical to seawater for major components, and local particles emitted from various anthropogenic activities (cf. Chen et al. 1997; Gao et al. 1997; Hong et al. 1998). The analysis of fly-ash samples from power station chimnies in North China shows an average composition of 0.3%–0.6% for Na (unpublished data). If we use a simple three-end-member mixing model including local source (X_1), long-distance transport (X_2) and sea salt (X_3), together with data of aerosol mass, Al (%) and Na (%) to substitute into the Eq. (3), the calculation is simplified to

$$\begin{bmatrix} 1.0 & 1.0 & 1.0 \\ 0.5 & 7.5 & 0 \\ 0.2 & 1.5 & 30.8 \end{bmatrix} \begin{bmatrix} X_1 \\ X_2 \\ X_3 \end{bmatrix} = \begin{bmatrix} 1.0 \\ Y_2 \\ Y_3 \end{bmatrix}. \tag{4}$$

See Table 5 for the end-member compositions. Again, data in Figs. 5–7 support the application of this simple mixing model for marine atmosphere at Qianliyan, for example, plot of Al against Na. At Qingdao samples show an end-member composition of 0.5%–1.0% for Al when the aerosol level and sea salt component is low, indicating the situation of fly-ash dominance (Fig. 6). This implies that local emissions have an important influence on the composition of aerosols, and an elaborate approach has to be adopted for source identifications.

To simplify the calculation, we normalized a_{11} to a_{13} and Y_1 by aerosol concentrations, hence $a_{1j} = 1.0$ and

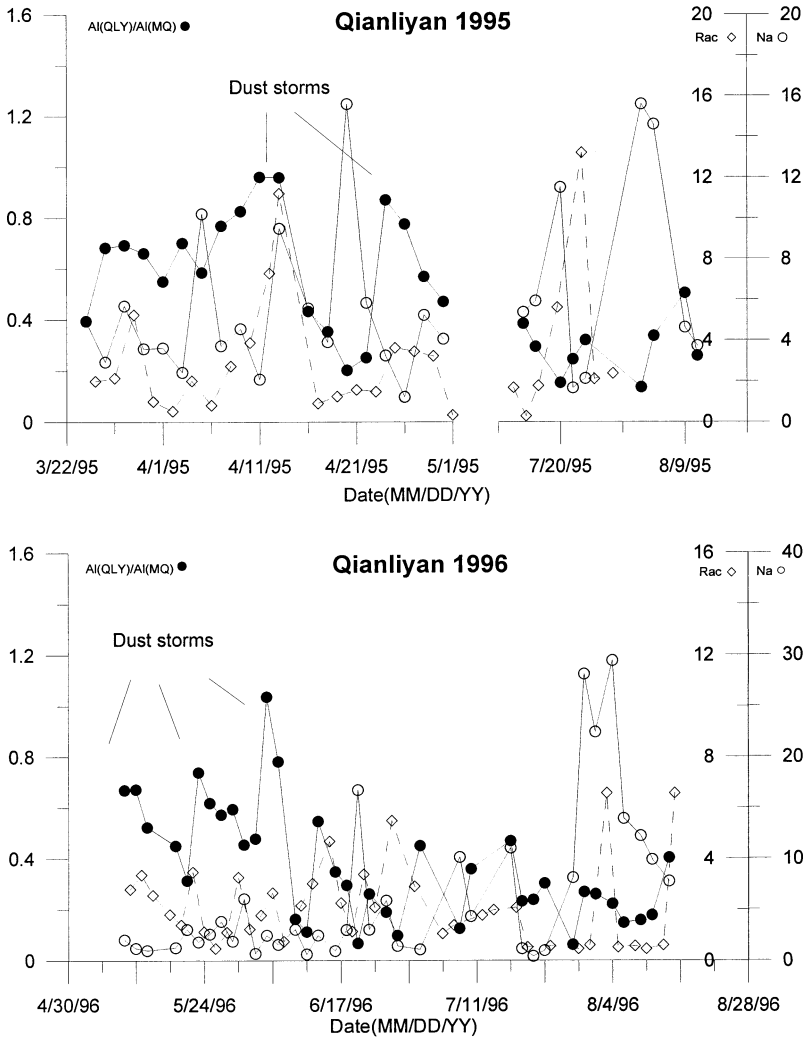

FIG. 8. Distribution of aerosol Al, Na, and RAC at Qianliyan in 1995 and 1996 measurements. The figure shows the ratio of Al [Al (QLY)] to [Al (MQ)], together with air-volume-based concentrations (μg m^{-3}) of RAC and percentage levels (%) of Na. Note that in late winter (Mar) the Al (QLY)/Al (MQ) ratio is relative low, averaging 0.5, with considerable contribution from anthropogenic emission (e.g., RAC). The value of Al (QLY)/Al (MQ) approaches 1.0 in spring when episodic dust storms pass through over the Yellow Sea, indicating dominance of crustal aerosols. Sea salt and anthropogenic contributions to aerosols can be considerably reduced by the high crustal materials in atmosphere when the cold fronts dominate, but become the major components in the nonstorm period in summer.

$Y_1 = 1.0$. The a_{2j} and a_{3j} represent the percentage concentration of Al and Na for local source (X_1), crustal materials from desert (X_2) and sea salt (X_3), respectively. The Y_2 and Y_3 are observed percentage concentrations for Al and Na at Qianliyan. Since we are interested in the proportion of various source materials in marine aerosols (i.e., Yellow Sea), we use reference index (i.e., Al and Na) for source identifications and omit the minor input of trace metals. The incorporation of RAC and RAS as end-member targets gives a very similar result, the end-member compositions of source (e.g., Minqin) and recipient (e.g., Qianliyan) are least defined, however. In this simple three-end-member mixing model, the end-member composition for crustal materials in desert (X_2) was from the measurements at Minqin, sea salt end-member (X_3) was from the stoichiometric composition of Na in seawater, and Al was assumed to be negligible. The end-member composition for local source (X_1), which is approached through the extrapolation of Na-Al (%) plot, Na and Al against aerosol concentration from Qingdao and Qianliyan (Figs. 6 and 7), is most difficult to define. The local source end-member composition of Na and Al in Table 5 corresponds, however, well to the data of fly-ash of fossil

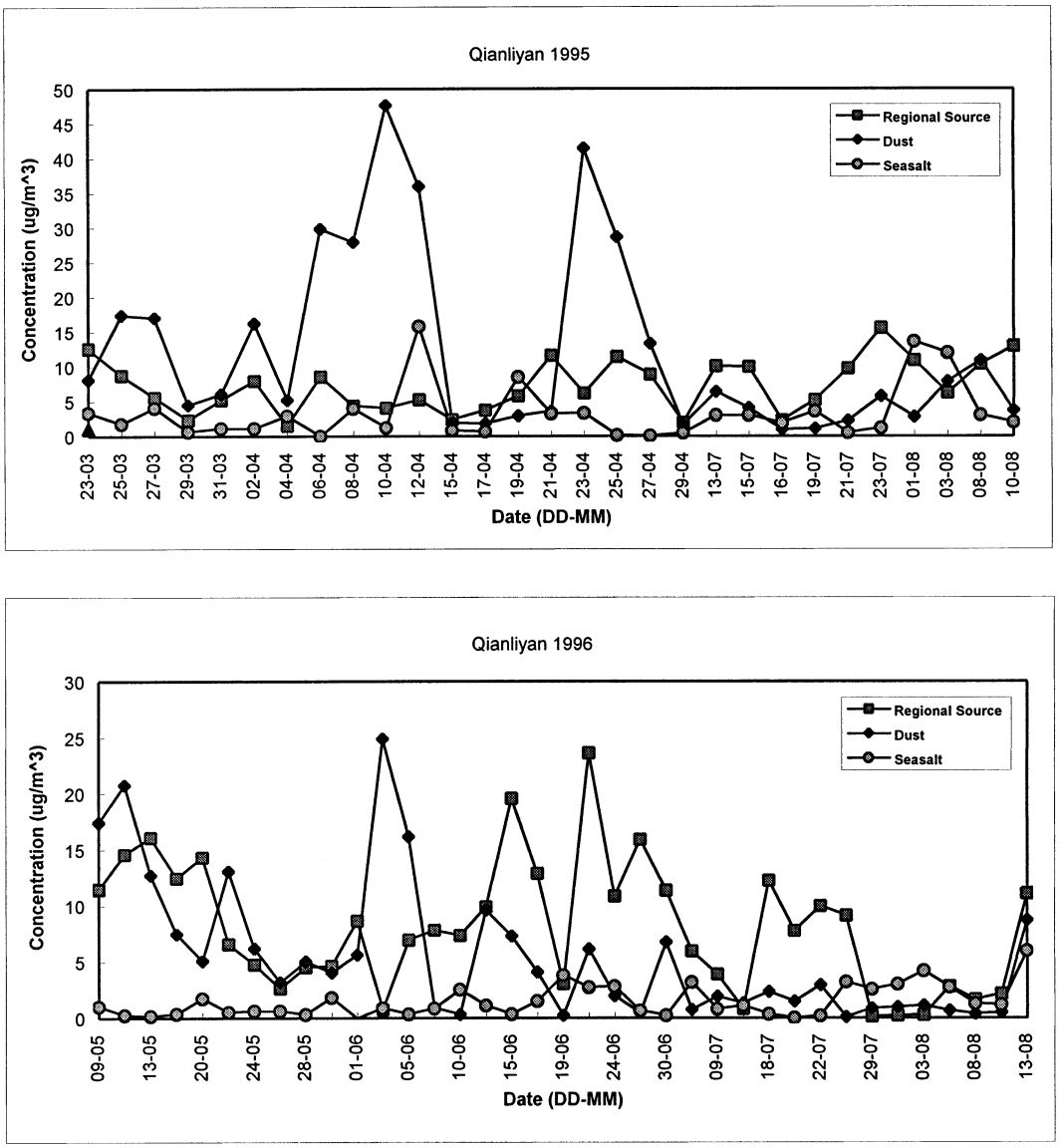

FIG. 9. Output of the three-end-member mixing model, which shows the levels of regional source, long-distance dust transport, and sea salt at marine atmosphere over the Yellow Sea in 1995 (upper panel) and 1996 (lower panel). The percentage contribution of end members in Eq. (4) is multiplied by the aerosol loadings to give an estimate of concentration in units of $\mu g\ m^{-3}$. Note that the peak concentrations of crustal materials correspond well to the cold front events over the Yellow Sea in spring, whereas the high level of aerosols in summer is from the contribution of regional source and sea salt.

fuel combustion, 0.15%–2.6% for Al and 0.1%–0.6% for Na (Wang and Yang 1984; Yang et al. 1987; Finkelman 1993; Wang et al. 1996; Shi et al. 2000; unpublished data).

To test the sensitivity of the model output relative to parameterization, the model was first run with different parameter inputs. It was found that the percentage contribution of crustal aerosols was not significantly (~15%–20%) affected by a twofold change for local source end-member and 50% for crustal end-member (data not shown). The results of data simulation are given in Fig. 9 for Qianliyan samples in 1995 and 1996, respectively, and several characters can be identified.

1) Long-distance transport of desert crustal materials has a significant impact on the aerosol composition in the Yellow Sea. The episodic increase of dust component may reach up to 80%–90% of total aerosol concentrations in spring, which compares well in time and space with the dust storms in source region. In summer, crustal input reduces dramatically over the Yellow Sea.

2) Local source material is a considerable component of aerosols at the Yellow Sea over the observation periods, owing to its downwind location to a strong emission source (e.g., northeast China). The local source is ~20%–40% in average in spring, when a strong input flux of cold fronts from desert region takes place, but increases up to 70%–80% in summer.
3) Sea salt represents a minor component (~10%) relative to other two fractions in spring, it becomes the dominant component in summer and contributes up to 60%–80% for observed aerosol mass, following the expiry of dust storms and reduction of anthropogenic emission in summer compared to spring and winter.

4. Summary and concluding remarks

The dataset of this study indicate that a close coupling of aerosol compositions exists between desert region (i.e., Minqin) and marine recipient (e.g., Yellow Sea) in East Asia. The percentage concentration of major inorganic components (e.g., Al, Ca, Mg, K, and Na) is considerably stable at the desert region, though the aerosol levels can be different by five- to tenfold between dust storms and nondust conditions. Aerosol samples from the Yellow Sea show much lower level but a considerable variability compared to the upwind desert area, presumably due to the remote location and an increased contribution from sea salt and/or anthropogenic emission. It was found that coastal marine atmosphere (e.g., Yellow Sea) responds to the dust storms in northwest China by a dramatic increase in aerosol levels and percentage concentration of crust-dominated elements. For instance, the contribution in percentage of dust component may account for 80%–90% of total aerosol mass when the cold fronts pass over across the Yellow Sea, such crustal aerosols may considerably reduce the contributions in percentage from sea salt and local source. The anthropogenic and sea salt aerosols become the dominant components in summer, when the dust storms in deserts and the Gobi are expired and southeast monsoon starts in the western Pacific Ocean.

Given that desert and Gobi cover an area of 1.3×10^6 km^2, which is threefold larger than the loess plateau (0.4×10^6 km^2) located downwind side at lower elevation, it can be expected that desert–Gobi is likely the main and original source region of the crustal aerosols over the North Pacific. Most of the reported dust storms the from meteorological agency are also initiated from desert region of northern China (cf. Table 4 and Fig. 1). Our field observation and sample analysis support this hypothesis. Following the national effort of afforestation and soil/water conservation, the initiation of dusts from Loess Plateau has been reduced in recent years, whereas regional desertization would result in an enhancement of injection of crustal particles into the atmosphere from desert/Gobi in spring, and transport to the ocean.

Acknowledgments. This study was funded by the Natural Science Foundation of China (Grant 49525609) and Ministry of Science and Technology (Grant G19990437-05). We thank Dr. K. N. Liou and the anonymous reviewers of the *Journal of the Atmospheric Sciences* for their very helpful review comments, which greatly improved the original manuscript.

REFERENCES

Carmichael, G., Y. Zhang, L. L. Chen, M. S. Hong, and H. Ueda, 1996: Seasonal variation of aerosol composition at Cheju Island, Korea. *Atmos. Environ.,* **30,** 2407–2416.

Chen, L. L., and Coauthors, 1997: Influence of continental outflow events on the aerosol composition at Cheju Island, South Korea. *J. Geophys. Res.,* **102,** 28 551–28 574.

Chester, R., and G. F. Bradshaw, 1991: Source control on the distribution of particulate trace metals in the North Sea atmosphere. *Mar. Pollut. Bull.,* **22,** 30–36.

——, M. Nimmo, G. R. Fones, S. Keyse, and J. Zhang, 2000: Trace metal chemistry of particulate aerosols from the UK mainland coastal rim of the NE Irish Sea. *Atmos. Environ.,* **34,** 949–958.

Chung, Y. S., 1992: On the observations of yellow sand (dust storms) in Korea. *Atmos. Environ.,* **26,** 2743–2749.

Countess, R. J., 1990: Interlaboratory analyses of carbonaceous aerosol samples. *Aerosol Sci. Technol.,* **12,** 114–121.

Finkelman, R. B., 1993: Trace and major elements in coal. *Organic Geochemistry: Principals and Applications,* M. H. Engel and S. A. Macko, Eds., Plenum Press, 593–607.

Friedlander, S. K., 2000: *Smoke, Dust and Haze—Fundamentals of Aerosol Dynamics.* 2d ed. Oxford University Press, 407 pp.

Gao, Y., R. Arimoto, R. A. Duce, D. S. Lee, and M. Y. Zhou, 1992: Input of atmospheric trace elements and mineral matter to the Yellow Sea during the spring of a low-dust year. *J. Geophys. Res.,* **97,** 3767–3777.

——, and Coauthors, 1997: Temporal and spatial distributions of dust and its deposition to the China Sea. *Tellus,* **49B,** 172–189.

Guieu, C., R. Chester, M. Nimmo, J. M. Martin, S. Guerzoni, E. Nicolas, J. Mateu, and S. Keyse, 1997: Atmospheric input of dissolved and particulate metals to the northwestern Mediterranean. *Deep-Sea Res. II,* **44,** 665–674.

Haswell, S. J., 1992: *Practical Guide to Chemometrics.* Marcel Dekker, 5–37.

Hong, G. H., S. H. Kim, D. B. Yang, and G. H. Lim, 1998: Atmospheric input of trace metals over the Yellow Sea: Shipboard results, April 1995. *Health of the Yellow Sea,* G. H. Hong, J. Zhang, and B.-K. Park, Eds., The Earth Love Publication Association, 211–235.

Kim, Y. P., J. H. Lee, N. J. Baik, J. Y. Kim, S. G. Shim, and C. H. Kang, 1998: Summertime characteristics of aerosol composition at Cheju Island, Korea. *Atmos. Environ.,* **32,** 3905–3915.

Liu, C. L., 1997: Transport of particulate heavy metals to the China Sea via river and atmosphere (in Chinese). M.S. thesis, Dept. of Marine Chemistry, Ocean University of Qingdao, 105 pp.

Ministry of Geology and Mineral Resources, 1986: *Preparation and Analysis of Geochemistry Statndards* (in Chinese). Geoscience Press, 358 pp.

Parungo, F., C. Nagamoto, M. Y. Zhou, A. D. A. Hansen, and J. Harris, 1994: Aeolian transport of aerosol black carbon from China to the ocean. *Atmos. Environ.,* **28,** 3251–3260.

Shi, L. M., X. C. Xu, H. Y. Qi, C. F. You, and C. H. Chen, 2000: Mechanism of FGD under medium temperature and steam activation of fly ash-lime (in Chinese). *Environ. Sci.,* **21,** 25–28.

Wang, A. P., and S. L. Yang, 1984: Element composition and fly ash (<10 μm) in atmosphere of Beijing (in Chinese). *Environ. Sci.*, **5,** 14–17.

Wang, Q. C., Q. C. Shao, S. L. Kang, C. H. Zhou, Z. G. Wang, S. T. Zhou, and D. M. Fu, 1996: Nine trace elements in the fly-ash of coal combustion (in Chinese). *Environ. Sci.*, **17,** 18–20.

Yang, S. J., and Coauthors, 1987: Source and character of aerosols in Beijing and Tianjin (in Chinese). *Acta Sci. Circumstantiae,* **17,** 412–422.

Zhang, D. Z., and Y. Iwasaka, 1999: Nitrate and sulfate in individual Asian dust-storm particles in Beijing, China in spring of 1995 and 1996. *Atmos. Environ.*, **33,** 3213–3223.

Zhang, J., Z. G. Yu, S. M. Liu, H. Xu, Q. B. Wen, B. Shao, and J. F. Chen, 1997: Dominance of terrigenous particulate organic carbon in the high-turbidity Shuangtaizihe Estuary. *Chem. Geol.*, **138,** 211–219.

——, S. Z. Chen, Z. G. Yu, C. S. Wang, and Q. M. Wu, 1999: Factors influencing changes in rainwater composition from urban versus remote regions of the Yellow Sea. *J. Geophys. Res.*, **104,** 1631–1644.